Atherosclerosis 210 (2010) 388–391

Contents lists available at ScienceDirect

Atherosclerosis

journal homepage: www.elsevier.com/locate/atherosclerosis

Rapid communication

Evaluation of translocator protein quantification as a tool for characterising macrophage burden in human carotid atherosclerosis

J.L.E. Bird[a,b,*], D. Izquierdo-Garcia[b], J.R. Davies[c], J.H.F. Rudd[c], K.C. Probst[b], N. Figg[c], J.C. Clark[b], P.L. Weissberg[c], A.P. Davenport[a], E.A. Warburton[d]

[a] Clinical Pharmacology Unit, Addenbrooke's Hospital, Hills Road, Cambridge CB2 0QQ, United Kingdom
[b] Wolfson Brain Imaging Centre, Addenbrooke's Hospital, Hills Road, Cambridge CB2 0QQ, United Kingdom
[c] Division of Cardiovascular Medicine, Addenbrooke's Hospital, Hills Road, Cambridge CB2 0QQ, United Kingdom
[d] Clinical Neurosciences, University of Cambridge, Addenbrooke's Hospital, Hills Road, Cambridge CB2 0QQ, United Kingdom

ARTICLE INFO

Article history:
Received 20 May 2009
Received in revised form
18 November 2009
Accepted 25 November 2009
Available online 4 December 2009

Keywords:
Atherosclerosis
[3H]DAA
[3H](*R*)-PK11195
Peripheral benzodiazepine receptor
Translocator protein
Macrophage
Inflammation

ABSTRACT

Macrophage presence within atherosclerotic plaque is a feature of instability and a risk factor for plaque rupture and clinical events. Activated macrophages express high levels of the translocator protein/peripheral benzodiazepine receptor (TSPO/PBR). In this study, we investigated the potential for quantifying plaque inflammation by targeting this receptor. TSPO expression and distribution in the plaque were quantified using radioligand binding assays and autoradiography. We show that cultured human macrophages expressed 20 times more TSPO than cultured human vascular smooth muscle cells (VSMCs), the other abundant cell type in plaque. The TSPO ligands [3H](*R*)-1-(2-chlorophenyl)-N-methyl-(1-methylpropyl)-3-isoquinoline carboxamide ([3H](*R*)-PK11195) and [3H]N-(2,5-dimethoxybenzyl)-N-(5-fluoro-2-phenoxyphenyl)acetamide ([3H]-DAA1106) bound to the same sites in human carotid atherosclerotic plaques *in vitro*, and demonstrated significant correlation with macrophage-rich regions. In conclusion, our data indicate that radioisotope-labelled DAA1106 has the potential to quantify the macrophage content of atherosclerotic plaque.

1. Introduction

Atherosclerosis is a chronic inflammatory disease of the arterial wall. Vulnerable or rupture-prone plaques are usually identified after clinical events such as myocardial infarction or stroke have occurred [1]. Macrophages are prominent in ruptured plaques suggesting that inflammation is a marker of vulnerability [2]. Inflammation is difficult to quantify with current imaging techniques (angiography, CT, MRI), which focus on the degree of stenosis rather than the composition of the atherosclerotic plaque.

Positron emission tomography (PET) imaging has the potential to selectively target and quantify inflammatory cells non-invasively with appropriate ligands. [18F]-fluorodeoxyglucose (FDG) can quantify carotid artery inflammation accurately [3–6], but is taken up avidly by the myocardium, so for coronary artery atherosclerosis imaging there is a need for radiotracers that are more selective for macrophages. The translocator protein/peripheral benzodiazepine receptor (TSPO/PBR) is highly expressed in the macrophage [7]. A number of ligands have been developed for the TSPO and the isoquinoline carboxamide PK11195 has been extensively characterised [8,9]. However, for *in vivo* imaging PK11195 demonstrates a low signal-to-noise ratio and high levels of non-specific binding [9–11]. The aryloxyanilide family of PBR-selective ligands [12] demonstrate superior binding characteristics for the TSPO [13]. In our study, we have evaluated the potential of both PK11195 and DAA1106 in the quantification of TSPO expression in the human atherosclerotic plaque.

2. Materials and methods

2.1. Ex vivo plaque collection and processing

Atherosclerotic plaques were obtained from six patients undergoing carotid endarterectomy (mean age ±SD 69 years ±2.8; range 64–72 years, 5 males and 1 female) and processed blinded to patient demographics. Tissue sections of 30 μm were frozen at −70 °C until required. All patients gave written, informed consent and the study was approved by the regional research ethics committee in Cambridge, UK.

* Corresponding author at: Box 65, Wolfson Brain Imaging Centre, Addenbrooke's Hospital, Cambridge CB2 0QQ, United Kingdom. Tel.: +44 1223 746463; fax: +44 1223 331826.
E-mail address: jleb2@wbic.cam.ac.uk (J.L.E. Bird).

0021-9150
doi:10.1016/j.atherosclerosis.2009.11.047

2.2. Binding assay

Receptor binding assays were performed on cultured, lipopolysaccharide-activated human blood-derived monocytes and cultured human VSMCs explanted from healthy arteries [14,15]. Briefly, [^{3}H](*R*)-PK11195 (3.15 TBq/mmol, 37 MBq/mL) (Amersham Bioscience, Amersham, UK) was used at 1–24 nM in saturation experiments. Saturation curves and Scatchard plots were generated from three separate experiments to produce values for receptor density (B_{max}) and the dissociation constant (K_D) (PRISM software, Graphpad Software Inc., La Jolla, CA, USA).

2.3. Autoradiography

Fresh frozen tissue sections were processed for receptor autoradiography. Sequential sections were incubated in [^{3}H](*R*)-PK11195 or [^{3}H]-DAA1106 (2.81 TBq/mmol, 74 MBq/mL) (Amersham Bioscience, Amersham, UK) according to published techniques [14]. Briefly, tissue sections were incubated in 5 nM [^{3}H](*R*)-PK11195 or 0.25 nM [^{3}H]-DAA1106 for 50 min. Non-specific binding was determined by the inclusion of 10 μM unlabelled ligand. Tissue sections and a tritium standard (Amersham Bioscience, Amersham, UK) were exposed to autoradiography screens for 7–14 days, imaged using a phosphor imager (PerkinElmer Inc., Waltham, MA, USA) and analysed with OptiQuant software (Packard Instruments Co., Meriden, CT, USA). Regional radioactivity was standardised using tritium standards (Amersham Bioscience, Amersham, UK).

2.4. Planimetry

Specific binding images were generated by automatically co-registering non-specific binding images to total binding images using VTK Cisg Registration Toolkit (VTKCisg, London, UK), then subtracting the non-specific binding images from total binding images using a MatLab™ script (MathWorks Inc., Cambridge, UK). Quantification of specific PK11195 and DAA1106 binding and CD68 immunohistochemical staining in images was performed using MatLab™.

2.5. Immunohistochemistry

Immunohistochemical staining was performed on adjacent sections using the EnVision system™ (Dako, Ely, UK). Macrophages were identified using an antibody to CD68 and non-specific expression was assessed by replacing CD68 antibody with isotype-specific IgG antibody in the absence of counterstain to facilitate planimetry. Activated pro-inflammatory and alternatively activated macrophages were identified using antibodies against tumour necrosis factor receptor type 1 (TNFR1) and CD163, respectively.

2.6. Statistics

Results are expressed as means and standard errors (SEM). The significance of correlations between samples was calculated using Spearman's ρ with SPSS™ software (SPSS Inc., Chicago, IL, USA). Statistical significance was set at the 5% level.

3. Results

Using [^{3}H](*R*)-PK11195 (the most extensively characterised TSPO ligand) we characterised TSPO expression on the two most abundant cell types present in the atherosclerotic plaque, VSMCs and macrophages. A high affinity binding site for PK11195 was identified on both blood-derived, activated macrophages and VSMCs; this site was 20-fold more abundant on the macrophages (Table 1, Fig. 1A and B).

Table 1
Comparison of TSPO receptor binding characteristics on activated, blood-derived macrophages and vascular smooth muscle cells. Receptor binding assays were performed with [^{3}H](*R*)-PK11195 as previously described in Section 2.

Cell type	Dissociation constant (K_D) (nM)	Receptor number (B_{max}) (fmol/mg)
Macrophages	3.656 ± 1.145	8,836 ± 841.2
VSMCs	5.49 ± 0.618	417.4 ± 16.3

Values expressed as mean ± SEM; $n = 3$.

The spatial localisation of [^{3}H](*R*)-PK11195 and [^{3}H]-DAA1106 binding to human atherosclerotic plaques was determined *in vitro*. Specific binding sites for [^{3}H](*R*)-PK11195 and [^{3}H]-DAA1106 (Fig. 1C and D and supplementary data Figs. 1–6A and B) were identified by subtraction of the non-specific binding images from the paired total binding images. Specific binding in these areas was quantified by measuring pixel intensity. PK11195 and DAA1106 signal demonstrated a significant correlation ($r = 0.828$, $p = 0.041$) (Table 2).

The expression of the macrophage marker CD68, was determined in adjacent tissue sections and demonstrated a punctuate pattern in the shoulder and cap regions (Fig. 1E; supplementary data, Figs 1C and 2C, inset regions) which was absent in isotype IgG control sections (Fig. 1F) and co-localised with both PK11195 and DAA1106 specific binding. Quantification of CD68 signal by planimetry enabled correlation with specific PK11195 and DAA1106 binding. The necrotic core of some plaques demonstrated CD68 expression (e.g. supplementary data, Figs. 2 and 3, arrowed regions) in the absence of IgG isotype control signal; these did not demonstrate specific [^{3}H](*R*)-PK11195 and [^{3}H]-DAA1106 binding. This was anticipated, because neither ligand could be expected to bind to dead cells. Adjacent tissue sections were stained with haematoxlyin and eosin (data not shown) to facilitate delineation of the necrotic core by blinded visual assessment. Exclusion of the necrotic core region from the CD68, PK11195 and DAA1106 images resulted in a significant correlation between DAA1106 and CD68 expression ($r = 0.94$, $p = 0.0048$) but not between PK11195 and CD68 ($r = 0.657$, $p = 0.156$).

TNFR1 is expressed in inflammatory macrophages and this receptor was present in CD68-rich regions, although with generally low expression levels (supplementary data, Figs. 1–6G). CD163 is a marker of alternatively activated macrophage phenotype and had more extensive, punctuate expression in CD68-rich regions (supplementary data, Figs. 1–6H). The relative proportions of these two activation markers varied considerably between plaques.

Table 2
Correlation of [^{3}H](*R*)-PK11195 and [^{3}H]-DAA1106 binding with CD68 expression. Specific binding of [^{3}H](*R*)-PK11195 and [^{3}H]-DAA1106 were derived as previously described. CD68 microscopy images were digitized and co-registered to autoradiography images. Quantification of specific PK11195 and DAA1106 binding and CD68 immunohistochemical staining in images was performed using MatLab™. DAA1106 signal was significantly correlated with CD68 expression.

Specific ligand/epitope expression	Mean	*P* value
[^{3}H](*R*)-PK11195 (DLU)	762927.0 ± 173369.8	<0.05*
[^{3}H]-DAA1106 (DLU)	285294.4 ± 56277.7	<0.005**
CD68 (% area)	17.4 ± 4.7	

[^{3}H](*R*)-PK11195 and [^{3}H]-DAA1106 values are presented as digital luminescence units (DLU).

* Significant correlation with [^{3}H]-DAA1106 signal.

** Significant correlation with CD68 expression. Values expressed as mean ± SEM; $n = 6$.

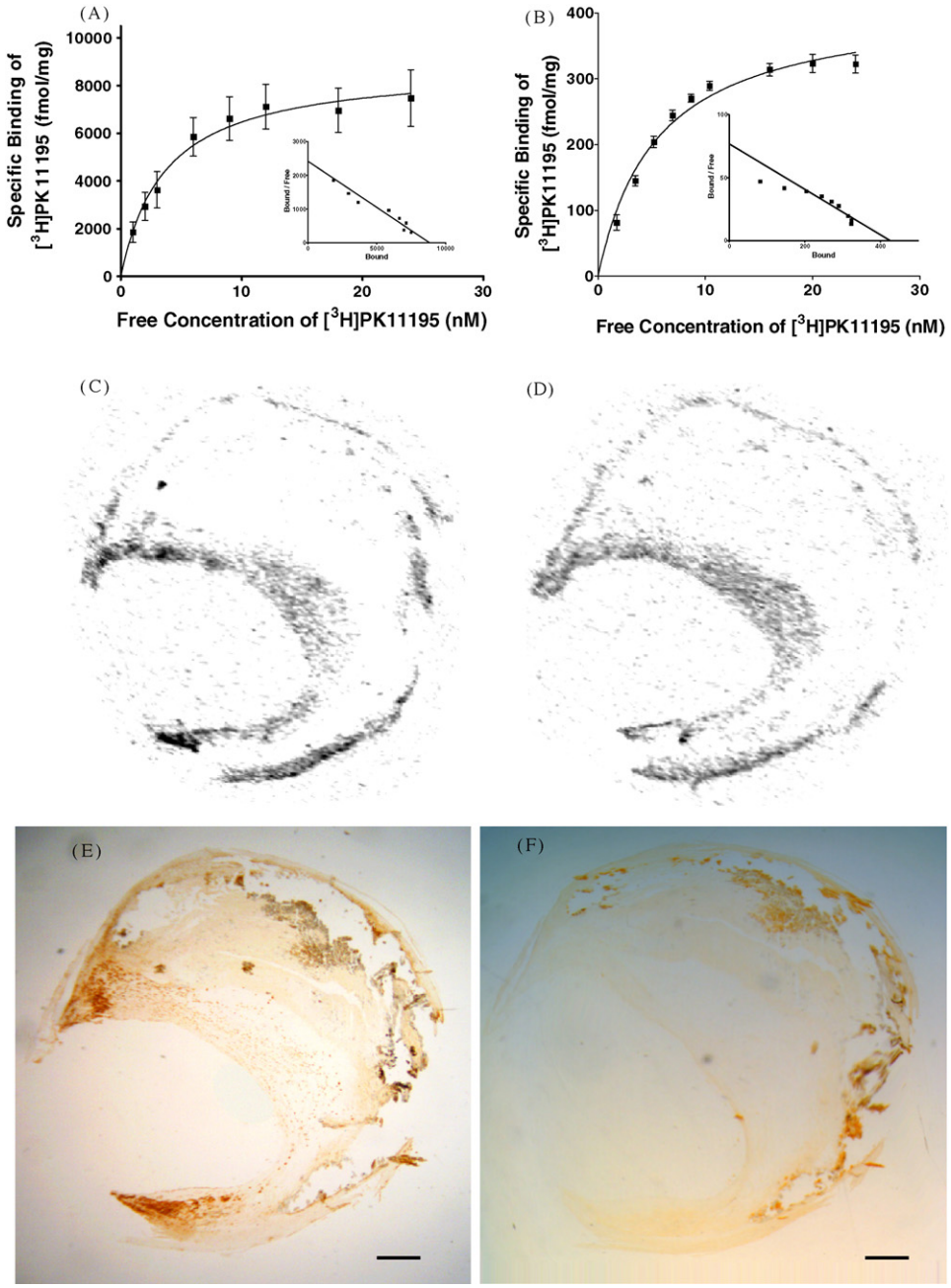

Fig. 1. Quantification of translocator protein (TSPO) in cultured cells, with co-localisation of TSPO and macrophage presence in a carotid endarterectomy tissue section from a single patient. Saturation and Scatchard plots of [^{3}H](*R*)-PK11195 binding in cultured, blood-derived monocytes (A) and vascular smooth muscle cells (B). Specific binding of [^{3}H](*R*)-PK11195 (C) and [^{3}H]-DAA1106 (D) in atherosclerotic vessel. Total and non-specific binding were obtained by autoradiography and specific binding was obtained by subtracting non-specific binding from total binding. Immunohistochemical staining of macrophages with antibody to CD68 (E). Microscopy images were digitized, co-registered to autoradiography images and quantified. Control sections (isotype-specific IgG antibody) showed negligible staining (F). Bar = 1 mm.

4. Discussion

In this study we have shown for the first time that the *in vitro* specific binding of [^{3}H]-DAA1106 in human atherosclerotic plaques demonstrates the same topography as that of [^{3}H](*R*)-PK11195. We also demonstrate that TSPO/PBR expression in cultured human macrophages is considerably higher than in VSMCs. In addition, after exclusion of redundant necrotic cores from analysis, we show a significant correlation between macrophage presence in the fibrous cap and the binding of [^{3}H]-DAA1106. These findings indicate that TSPO expression in plaque macrophages represents a potential target for the *in vivo* quantification of carotid plaque inflammation using non-invasive PET scintigraphy.

The derivation of TSPO receptor binding data from atherosclerotic plaques is problematic due to the size of lesion and heterogeneous mix of cells. Therefore, we quantified TSPO expression on cultured cell populations using PK11195 which is the best characterised TSPO ligand. Mature macrophages were produced from blood-derived monocytes. The density of TSPO expression (B_{max}) on these macrophages was approximately 20-fold higher than that on VSMCs, demonstrating considerable discrimination between the two major cell types present in the plaque. Both cell types had a single, high affinity binding site consistent with the presence of the TSPO receptor, supporting the study of Fujimura et al. [16]. Fujimura calculated a TSPO abundance (B_{max}) of 1.6 pmol/mg protein in intact, *in vitro* atheroma,

using a K_D value of 18 nM derived from cultured human blood monocytes [10]. This B_{max} value lies between our values for the two cell types and is consistent with a mixed population of high (macrophage) and low (VSMC) TSPO expressing cells (Table 1).

PK11195 has previously shown some binding in the necrotic core of human plaques (data not shown) and poor discrimination between murine inflamed and stable atherosclerotic plaques [17], suggesting poor *in vivo* binding. Thus, there is a need for TSPO ligands with high selectivity for the TSPO and a lower non-specific binding. The aryloxyanilide family of TSPO-selective ligands [12] have superior TSPO binding characteristics compared to PK11195 [13]. In our study, PK11195 and DAA1106 specific binding and CD68 expression were assessed on sequential sections. PK11195 and DAA1106 specific binding had statistically significant topographical co-incidence within each plaque, which was largely restricted to the shoulder and cap regions. Thus, both ligands demonstrated selectivity towards TSPO in macrophage-rich regions.

The plaques used in this study had considerable morphological heterogeneity. The macrophage-specific protein CD68 was present as punctuate foci in the shoulder and cap regions of the carotid plaques. Where punctuate CD68 expression was present in the necrotic core of some plaques, these regions also exhibited specific binding of PK11195 and DAA1106. In other plaques, a diffuse expression was present which did not exhibit specific radioligand binding, suggesting that this was not related to viable macrophages. IgG isotype control binding was minimal in all the necrotic cores examined. Examination of the macrophage phenotype suggested the presence of both classically activated, pro-inflammatory macrophages (TNFR1 expression) and alternatively activated, anti-inflammatory macrophages (CD163 expression). CD163 is associated with the clearance of proinflammatory haemoglobin and the resolution of wound inflammation through production of IL-10. Thus, the presence of CD163 expression in these plaques is consistent with resolution of inflammation after rupture of the plaque. The relative proportions of these two markers varied considerably between plaques, consistent with differences in time between plaque rupture and surgical removal of the plaque at endarterectomy. The impact of macrophage activation phenotype or differentiation (macrophages are the precursors of foam cells) on TSPO expression is currently unknown. The statistically significant correlation between CD68 and DAA1106 specific binding and the superior selectivity and binding affinity of DAA1106 for the TSPO suggest that this ligand should perform better in quantifying macrophage abundance by PET imaging in a clinical setting. The presence of both pro-inflammatory and anti-inflammatory macrophage phenotypes in these plaques highlights a potential drawback in the validation of PET ligands using *ex vivo* human clinical tissue. Further validation of this ligand for imaging the pre-rupture inflammatory phase of atherosclerosis is suggested, using preclinical models of disease with predictable morphology and pathogenesis.

Acknowledgements

This work was supported by the British Heart Foundation (JLEB, DI-G, and KCP [RG/03/013]; JRD, PLW and APD [PS/02/001]), the European Union (JCC [EC-FP6-project DiMI, LSHB-CT-2005-512146]) and the NIHR Cambridge Biomedical Research Centre (EAW, JHFR).

Appendix A. Supplementary data

Supplementary data associated with this article can be found, in the online version, at doi:10.1016/j.atherosclerosis.2009.11.047.

References

[1] Fuster V, Stein B, Ambrose JA, et al. Atherosclerotic plaque rupture and thrombosis. Evolving concepts. Circulation 1990;82:II47–59.
[2] Libby P, Geng YJ, Aikawa M, et al. Macrophages and atherosclerotic plaque instability. Curr Opin Lipidol 1996;7:330–5.
[3] Rudd JH, Myers KS, Bansilal S, et al. Atherosclerosis inflammation imaging with ^{18}F-FDG PET: carotid, iliac, and femoral uptake reproducibility, quantification methods, and recommendations. J Nucl Med 2008;49:871–8.
[4] Tawakol A, Migrino RQ, Bashian GG, et al. In vivo ^{18}F-flurodeoxyglucose positron emission tomography imaging provides a non-invasive measure of carotid plaque inflammation in patients. J Am Acad Cardiol 2006;48:1818–24.
[5] Rudd JHF, Warburton EA, Fryer TD, et al. Imaging atherosclerotic plaque inflammation with [^{18}F]-fluorodeoxyglucose positron emission tomography. Circulation 2002;105:2708–11.
[6] Tahara N, Kai H, Ishibashi M, et al. Simvastatin attenuates plaque inflammation: evaluation by fluorodeoxyglucose positron emission tomography. J Am Acad Cardiol 2006;48:1825–31.
[7] Zavala F, Haumont J, Lenfant M. Interaction of benzodiazepines with mouse macrophages. Eur J Pharmacol 1984;106:561–6.
[8] Banati RB. Visualizing microglia activation in vivo. Glia 2002;40:206–17.
[9] Chauveau F, Boutin H, Van Cam N, et al. Nuclear imaging of neuroinflammation: a comprehensive review of [^{11}C]PK11195 challengers. Eur J Nucl Med Mol Imag 2008;35:2304–19.
[10] Venneti S, Wang G, Wiley CA. The high affinity peripheral benzodiazepine receptor ligand DAA1106 binds to activated and infected brain macrophages in areas of synaptic degeneration: implications for PET imaging of neuroinflammation in lentiviral encephalitis. Neurobiol Dis 2008;29:232–41.
[11] Boutin H, Chauveau F, Thominiaux C, et al. ^{11}C-DPA-713: a novel peripheral benzodiazepine receptor PET ligand for in vivo imaging of neuroinflammation. J Nucl Med 2007;48:573–81.
[12] Chaki S, Funakoshi T, Yoshikawa R, et al. Binding characteristics of [^{3}H]DAA1106, a novel and selective ligand for peripheral benzodiazepine receptors. Eur J Pharmacol 1999;371:197–204.
[13] Venneti S, Wagner AK, Wang G, et al. The high affinity peripheral benzodiazepine receptor ligand DAA1106 binds specifically to microglia in a rat model of traumatic brain injury: implications for PET imaging. Exp Neurol 2007;207:118–27.
[14] Davenport AP, Kuc RE. Radioligand-binding and molecular-imaging techniques for the quantitative analysis of established and emerging orphan receptor systems. In: Davenport AP, editor. Receptor Binding Techniques. New Jersey: Humana Press; 2005. p. 93–120.
[15] Davies JR. Imaging and quantification of inflammation in atherosclerotic plaques using positron emission tomography. Ph.D. Thesis, University of Cambridge, 2007.
[16] Fujimura Y, Hwang PM, Trout H, et al. Increased peripheral benzodiazepine receptors in arterial plaque of patients with atherosclerosis: an autoradiographic study with [^{3}H]PK 11195. Atherosclerosis 2008;201:108–11.
[17] Laitinen I, Marjamäki P, Någren K, et al. Uptake of inflammatory cell marker [^{11}C]PK11195 into mouse atherosclerotic plaques. Eur J Nucl Med Mol Imag 2009;36:73–80.